# Road navigation using multiple dissimilar environmental features to bridge GNSS outages

Debbie Walter, Paul D. Groves, *University College London, UK*;
Bob Mason, Joe Harrison, Joe Woodward, Paul Wright, *Terrafix Ltd., UK*

## BIOGRAPHY

Debbie Walter is a PhD student at University College London (UCL) in the Engineering Faculty's Space Geodesy and Navigation Laboratory (SGNL). She is interested in robust multi-sensor integrated navigation and navigation techniques not reliant on GNSS. She has a MSci from Imperial College London in physics and has worked as an IT software testing manager.

Dr Paul Groves is a Lecturer (academic faculty member) at UCL, where he leads a program of research into robust positioning and navigation and is a member of SGNL. He joined in 2009, after 12 years of navigation systems research at DERA and QinetiQ. He is interested in all aspects of navigation and positioning, including multi-sensor integrated navigation, improving GNSS performance under challenging reception conditions, and novel positioning techniques. He is an author of more than 70 technical publications, including the book *Principles of GNSS, Inertial and Multi-Sensor Integrated Navigation Systems*, now in its second edition. He is a Fellow of the Royal Institute of Navigation and holds a bachelor's degree and doctorate in physics from the University of Oxford. (p.groves@ucl.ac.uk)

Dr Bob Mason is Chief Scientific Officer/Director of Terrafix Limited; integrators and designers of navigation and communications systems. A physics graduate from Imperial College London, he obtained his PhD in communications and neuroscience from Keele University in 1981 and was involved in design of complex systems at Marconi Space and Defence Systems before joining Terrafix in 1985. He is a chartered scientist and physicist and a member of the Institute of Physics. His research interests include novel navigation techniques, software defined radio (SDR) and cognitive systems.

Joe Harrison is principal radio frequency (RF) design engineer at Terrafix Ltd. He has been with Terrafix for thirty years and has worked on a variety of design and research projects including mobile network radios, GSM modems and radio modems. Before working for Terrafix Ltd he worked for Marconi Space and Defence and Marconi Secure Radio Systems working on a variety of electronic warfare (EW) and electronic countermeasures (ECM) projects.

Joe Woodward is software design engineer at Terrafix Ltd. He has been with Terrafix for seven years and has worked on a variety of design and research projects ranging from low-level embedded software and DSP algorithms through to high-level database and website design. Before working for Terrafix Ltd he worked for Icera Ltd (acquired nVidia Ltd) on their software defined radios (SDR) for cellular networks as part of the Silicon Design Team, which was responsible for world-leading SDR solutions using novel processor architecture, full custom silicon design and layout and industry-leading software tools.

Dr Paul Wright is a development engineer with Terrafix Ltd. He has degrees in physics and in electronics. Prior to working at Terrafix, he has many years experience designing and testing large reflector antennas for radar and satcomms systems. He moved to development in mobile data and navigation systems after work with satellite internet access systems and network management software. He is a chartered engineer, and member of the Institution of Engineering & Technology, and of the Institute of Physics.

## ABSTRACT

Many navigation techniques have now become so reliant on GNSS that there is no back-up when there is limited or no signal reception. If there is interference, deliberate jamming or spoofing, and/or blockage and reflection of the signals by buildings, navigation could be lost or become misleading. Other navigation techniques harness different technologies such as Wi-Fi, eLoran and inertial navigation. However, each of these techniques has its own limitations, such as coverage, degradation in urban areas or solution drift. Therefore there is a need for new navigation and positioning paradigms that may be integrated with GNSS to increase the reliability of the system as a whole.

This paper presents the results of a feasibility study to identify a set of novel environmental features that could be used for road navigation in the temporary absence or degradation of GNSS. By measuring these features during times of GNSS availability, a map can be produced. This map can be referred to during times of limited reception. The most feasible environmental features are identified, their potential for providing position information is quantified and various methods of combining these features are analysed. It was found across multiple test routes that it is possible to determine the position of a vehicle along a route using three sensors: barometer, magnetometer and a camera looking at road signs.

This work is relevant to any road application that requires resilient positioning. Examples include navigation and tracking of ambulances, fire, police and security vehicles;

high-value asset tracking; transport logistics; road-user charging and pay-as-you-drive insurance.

## 1. INTRODUCTION

Many navigation applications have now become solely reliant on Global Navigation Satellite Systems (GNSS) so that there is no backup for when the signals received from GNSS are limited or entirely unavailable [1]. Therefore if there is interference to the signal, navigation capabilities can be lost or become misleading. This interference could be caused deliberately or accidentally. The increasing use of "personal privacy" devices to defeat GNSS-based tracking has made short-range jamming more prevalent, whilst the increasing demand for radio spectrum could make adjacent channel interference a greater threat. GNSS performance can also be degraded in dense urban areas by blockage and reflection of the signals by buildings.

Where a robust and reliable position solution is required, it is necessary to combine GNSS with other technologies. All navigation and positioning techniques are based on one of two fundamental methods: position fixing and dead reckoning. Position fixing techniques, such as GNSS, determine position directly using identifiable external information, whereas dead reckoning measures the distance and direction travelled from a known starting point [2].

Dead-reckoning using inertial sensors works by integrating measurements from accelerometers and gyroscopes, can potentially be used for any application. However high-performance sensors are expensive and are generally reserved for use in applications such as UAV where navigation needs to be entirely self-contained. For road navigation, odometry, which measures the rotation of the vehicle's wheels, is also commonly used. This may be combined with a gyroscope for turn detection and accelerometers for detecting wheel slip. However, all dead-reckoning techniques suffer from the problem that the accuracy of the position solution degrades with time due to the accumulation of sensor errors. Therefore, dead-reckoning is commonly integrated with GNSS. GNSS constrains the growth of the dead-reckoning errors and complementarily dead-reckoning can bridge outages in the GNSS position solution [2]. However, dead-reckoning is only suitable for bridging short outages. For robustness against longer GNSS outages, alternative position fixing techniques are needed.

Position fixing systems can use either man-made signals or environmental features to provide the information they require to determine position [2]. Most signal-based systems use radio-waves and there are many alternatives to GNSS already. Most smartphones are capable of positioning using mobile phone and Wi-Fi signals, as well as GNSS. However, many "personal privacy" devices jam these signals as well as GNSS. Enhanced Long-range Navigation (ELoran) is difficult to jam, but is only available in a few countries (including the United Kingdom) and can exhibit large errors in urban areas due to re-radiation effects [3]. Navigation using broadcast signals of opportunity has been investigated [4] [5] [6], however, these techniques are not yet mature, whilst most other radio positioning techniques are designed for either air or indoor navigation. For these reasons radio-based signals have been excluded from the study but may still play a part in the final navigation solution.

For land navigation in particular, a new approach is therefore needed and environmental features provide a potential source of location information. These include buildings or parts thereof, signs, roads, rivers, terrain height, sounds, smells, and even variations in the magnetic and gravitational fields [2]. There is currently a lot of interest in visual navigation techniques for land vehicles [7] [8]. These technologies are being developed and are likely to be complementary to the feature matching discussed in this paper; however they will not be directly discussed in this study. All the environmental features will be integrated with dead reckoning and so provides robust positioning.

The overall solution is to place hardware within a batch of vehicles, comprising of multiple sensors, (the exact combination to be determined from the feasibility study) including a GNSS receiver and sensors for dead reckoning. Road map matching could also be included. During normal usage the GNSS receiver is used for positioning and a database is updated with the feature information from all the sensors accompanied by location stamps from the GNSS-based position solution. As the multiple vehicles travel around an area the database is built up for these routes. In the event that the GNSS receiver does not receive sufficient signals to maintain an accurate position, the database is called upon for navigation by environmental feature matching. In this scenario the sensors will continue to take measurements and by combining the knowledge of the last known location, dead reckoning and the sensor's outputs, the positioning algorithm will draw upon the database to estimate a positioning solution. This method is shown in **Figure 1** and **Figure 2**.

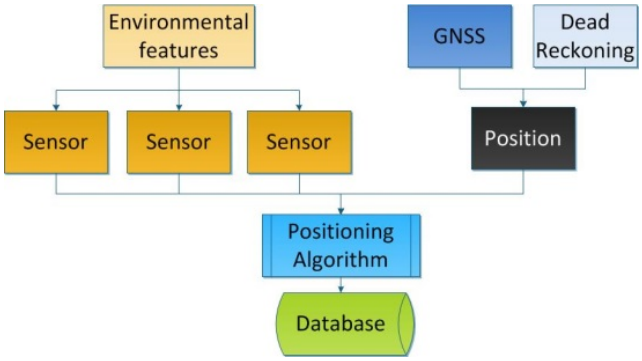


**Figure 1 -** Basic workflow mode for collecting data.

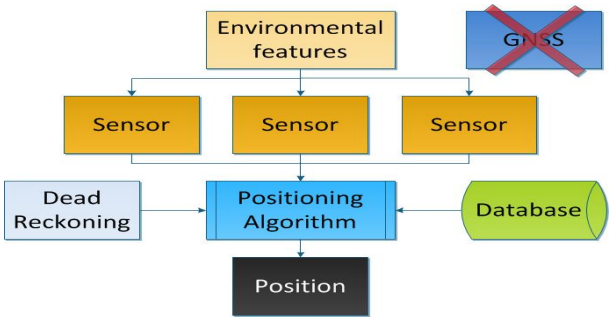


**Figure 2** - Basic workflow mode for navigation using collected data.

This navigation system relies upon the roads being travelled on a regular basis so that the 'maps' created from the sensor's outputs are kept up to date and therefore valid. The most likely users of this technology would be fleets of vehicles that can share the mapping information. To focus on a typical system, use in emergency vehicles was considered. Knowing your position is vital in an emergency vehicle and a system that incorporates a back-up to GNSS would be advantageous. The motivation for maintaining a continuous positioning solution is that, when moving within a complex environment, it is necessary to maintain the integrity of the current position. In emergency situations, delays are not acceptable and integrity is vital. There will be no point in time when the vehicle can be delayed to obtain a position fix.

Although this system will be designed with emergency service vehicles such as ambulances and police cars in mind, it could also be used in wider applications such as fleet management and tracking devices. Ultimately, crowd sourcing or cooperative techniques could be used to pool information from different vehicles equipped with the system. With a very large number of vehicles maintaining the feature database, the system could adapt to changes in the environment very quickly.

This paper presents the results of a feasibility study to determine which combination of environmental features could be used to create the proposed navigation system. Then it presents methods of combining the data from the different features to maximise the accuracy and precision of the navigation system. Phase 1 (Section 2) summarises an initial literature-based assessment of the different classes of environmental features. Section 3 presents a road experiment collecting data from multiple sensors. Phase 2 (Section 4) presents the cross correlation coefficients for sensors along the full routes covered in the road experiment. It also analyses a method of determining the similarity of a sequence of event for discrete features using an augmented Damerau-Levenshtein Distance technique (Section 5). Phase 3 (Section 6) analyses the road experiment data to determine if there is sufficient repeatability and unique information to identify the part of a route by comparing regions within two different rounds. Phase 4 (Section 7) introduces a scanning technique to predict a car's location by scanning along a section of road and estimating the cross correlation of the car at each location and producing a cross correlation profile. Phase 5 (Section 8) then describes methods for combining multiple features and how these can be weighted. Section 9 draws conclusions and finally, Section 10 sets out the next steps of the project.

To reliably achieve meters-level positioning across a range of different challenging environments, a paradigm shift is needed. We need to use as much information as we can cost-effectively obtain from many different sources in order to determine the best possible navigation solution in terms of both accuracy and reliability.

This new approach to navigation and real-time positioning in challenging environments requires many new lines of research to be pursued [9]. These include:

- How to integrate many different navigation and positioning technologies when the necessary expertise is spread across multiple organisations [10];
- How to adapt a multisensor navigation system in real-time to changes in the environmental and behavioural context to maintain an optimal solution [11];
- How to use 3D mapping to improve the performance of existing positioning technologies, such as GNSS, in dense urban areas [12] [13];
- How to obtain more information for positioning by making use of new features of the environment, the subject of this paper.

## 2. PHASE 1 – LITERATURE STUDY

### 2.1 Brainstorm Categories

A brainstorming exercise and a literature study were conducted to generate a list of possible environmental features that were assessed for the viability of each candidate using the current scientific literature. This is discussed in detail in our *ION GNSS+ 2013* paper [14] .

There were five categories that the brainstorm features were evaluated against:

- Temporal Variation (T)
- Practicality for use on road vehicle (Pra)
- Ambiguity (A)
- Precision (Pre)
- Coverage (C)

Continuous coverage is not required because the features are to be used in combination and integrated with dead reckoning techniques, such as odometry and inertial navigation.

### 2.2 The Features

15 different features were evaluated in the brainstorming exercise. All 15 are listed in **Table 1.** The environmental features are scored out of 5 for Temporal Variation (T), Practicality for use on road vehicle (Pra), Ambiguity (A), Precision (Pre) and Coverage (C) and total to give the overall score. The top few will be discussed in this section.

**Table 1 - Scores for features**

| Feature | T | Pra | A | Pre | C | Total |
|---|---|---|---|---|---|---|
| Road Signs | 5 | 4 | 3 | 4 | 4 | 20 |
| Terrain Height | 5 | 5 | 3 | 3 | 3 | 19 |
| Ambient Light | 4 | 5 | 2 | 3 | 3 | 17 |
| Vehicle Movement | 4 | 4 | 2 | 4 | 3 | 17 |
| Magnetic Field | 3 | 5 | 2 | 3 | 4 | 17 |
| Celestial | 3 | 3 | 5 | 1 | 3 | 15 |
| Road Texture | 3 | 4 | 2 | 4 | 2 | 15 |
| Scent | 2 | 5 | 3 | 2 | 2 | 14 |
| Temperature | 1 | 5 | 2 | 1 | 3 | 12 |
| Radioactivity | 2 | 5 | 2 | 2 | 1 | 12 |
| Gravity | 5 | 2 | 3 | 1 | 1 | 12 |
| Vehicle Speed | 1 | 4 | 1 | 2 | 3 | 11 |
| Environmental Sounds | 1 | 2 | 2 | 3 | 1 | 9 |
| Pulsar | 5 | 1 | 3 | 0 | 0 | 9 |
| Wind Speed | 0 | 4 | 2 | 2 | 0 | 8 |

### 2.2.1 Road signs

Text or symbols can be identified from the visual environment; this could be street signs, shop names or warning signs [15]. In the present context a sign was define as a sign from the British Government traffic signs website [16]. It should be noted that these traffic signs follow international road sign conventions and so techniques could easily be converted to work for signs from other countries. This could be expanded in future work to include other sign sets. **Figure 3** shows some examples of street signs in Great Britain. Consistency of text font and background colours will be an aid in the task of sign recognition.


**Figure 3** - Example road signs. Crown Copyright [16]

An issue with this technology could be that signs can be obscured from view by road furniture or other vehicles. Poor lighting conditions will also make it more difficult to read signs and especially make it challenging to distinguish different colours [17]. Another issue that could be encountered is that some signage is temporary such as when there are road works and this would affect the reliability of the road sign database.

### 2.2.2 Magnetic Field

Human-created magnetic fields are produced by numerous objects and devices in urban areas. These are considered magnetic anomalies and can be detected above the background of the Earth's magnetic field. The magnetic anomalies have been shown to provide a 'fingerprint' for the environment [18] but there will still be issues with temporal variation caused by fields created by cars etc.

### 2.2.3 Barometric Height

Terrain-referenced navigation (TRN) determines position by comparing a series of measurements of the height of the terrain below a vehicle with a database known as a digital terrain model (DTM) or digital elevation model (DEM) [2]. TRN has traditionally been used for air navigation but also more recently in underwater vehicles.

Land vehicles can be assumed to maintain a constant height above the road terrain but that there will likely be fluctuations in height along that road. A barometric altimeter may be used to measure variations in terrain height. Thus, in principle, TRN may be performed [19] [20]. However, as the vehicle travels much slower, a high-resolution database is needed to capture sufficient terrain height variation to determine position compared with traditional TRN. This can be circumvented if users build their own databases. However terrain height will not work if the terrain is entirely flat.

### 2.2.4 Ambient Light

There are two options for measuring the ambient light levels. One is to use a simple photo-diode that reads the intensity of the light. The other is to use a camera which has greater resolution but may give a more complex interpretation of the ambient light. Experimentation could show that the photo-diode gives sufficient information on the light intensity and that more complex measures are not needed.

A simple positioning method for exploiting ambient light is determining passage through a tunnel or under a bridge or a gantry. These cause sudden changes to light levels; therefore it will be necessary to incorporate a method calibrating the background light level changes that will change more slowly. These changes could be caused by broken cloud cover and shadowing due to travelling at different times of day.

### 2.2.5 Vehicle movement

Unique movements made by vehicles could be used to determine its position. These movements could be a vehicle going around a roundabout; this would produce a noticeable signal on the horizontal plane of an accelerometer. Other vehicle movements include speed restriction methods that involve a slalom manoeuvre in the road or speed bumps. An issue for the accelerometer is the speed that these actions are made at. As a signal, it will be more pronounced if it is taken at speed. It may be possible to mitigate this by averaging the signal.

## 3. ROAD EXPERIMENT

### 3.1 Motivation

The next step was to run an experiment, using a road vehicle. The aim of the experiment was to provide the data necessary to assess the viability of using dissimilar environmental features to bridge GNSS outages.


**Figure 5 -** Road types used in the road experiment. From top left clockwise: suburban, high speed road, rural and urban

### 3.2 Method

A set of sensors with a GNSS receiver were attached to a car and driven in closed loops around Stoke-on-Trent on multiple road types over multiple days. The loops were repeated three times on each day on four road types and then repeated over three consecutive days. **Figure 4** shows the four routes. A Vauxhall Insignia car (mid-range hatchback) was used for the experiment and can be seen in **Figure 6** and the sensors used can be seen in **Table 2**.

**Figure 6 -**Vauxhall Insignia used in the 1st car experiment, sensor unit can be seen on roof (red oval).

**Table 2- Sensors used in the road experiments**

| Sensor type | Sensor name | Feature |
|---|---|---|
| Accelerometer | ADXL345 | Road Texture |
| Air Quality | SEN01111P | Scent |
| Barometer | BMP180 | Terrain Height |
| Dust | GP2Y1010AU0F | Scent |
| GNSS & IMU | Xsens MTi-G | GNSS & DR |
| Light Sensors | ISL29125 | Ambient Light |
| Magnetometer | Terrafix inertial compass 10000/1 | Magnetic Field |
| Microphone | Phidgets1133 | Road Texture |
| Thermometer | Yocto-Temp | Temperature |
| Video Camera | Panasonic SDR-H81 | Road Signs |

The accelerometer, air quality sensor, barometer, dust sensor, light sensors and microphone interfaced with an Arduino microprocessor which outputted the signals from the sensors to a laptop. The Arduino sensors had a data rate of 20 measurements per second. The video recorder filmed the turning on of the IMU, Arduino, yocto-sensors and the Terrafix inertial compass to assist with synchronisation. There was an individual accelerometer (attached to the axel of the vehicle) for use in identifying road texture. There are also accelerometers that form part of the IMU and these were used for dead reckoning. **Table 3** shows the data rate of the sensors.

**Table 3 - Data rate for experiment's sensors**

| Sensor type | Data rate (measurements/s) |
|---|---|
| Arduino sensors | 20 |
| Yocto-sensors | 3 |
| Xsens | 100 |
| Terrafix inertial compass | 7 |

The onset of movement as recorded from the IMU was used to assist identifying the beginning of each circuit. During the car journeys there were two experimenters, one to drive the car and another to monitor the sensors. There was 5-10 minutes between each round, during this time the sensors would be turned off and then restarted. The equipment was designed for the outputs of the sensors to be post-processed.

The four classes of road were suburban, urban, rural and high speed road. The route taken and a view from Google Street View showing the general type of landscape travelled through can be seen in **Figure 4.**

A second road experiment was recently performed and this experiment travelled the same routes but had an improved synchronisation method where there was GPS receivers included with the Arduino, video camera and the IMU so that GPS time could be used as a constant for the different sensors. The results from both experiments are presented here. The light sensor data is from the second experiment and all other data is from the first.

## 4. PHASE 2 – WHOLE ROUTE ANALYSIS

The outputs from the sensors were evaluated initially for their cross correlation over the whole route. This assessed if the data from different runs but the same terrain were similar and thus had a high cross correlation. This is vital for this map-building method of navigation. This section deals only with sensors that produce continuous output. Section 5 will discuss discrete features.

### 4.1 Cross Correlation

Cross Correlation is a statistical method for determining similarity between two series' data. Cross Correlation is used in this section to determine how repeatable the measurements from a particular sensor are if the same journey is travelled multiple times.

The derivation of cross correlation [21] is below:

The two data series' can be presumed to be two random variables $X$ and $Y$. If $X$ and $Y$ are independent variables then the expected value of $XY$ can be given as:

$$E(XY) = E(X)E(Y) \tag{4.1}$$

The covariance of $X$, $Y$ or the moment of joint distribution of $X$ and $Y$ is defined as:

$$\begin{aligned}\mathrm{cov}(X,Y) &= E[(X-\mu_X)(Y-\mu_Y)] \\ &= E(XY) - E(X)E(Y)\end{aligned} \tag{4.2}$$

where $\mu$ is the mean of the relevant distribution.

Thus it can be deduced that if $X$ and $Y$ are independent then $E(XY) = E(X)E(Y)$ and so it follows that $\mathrm{cov}(X,Y) = 0$. If $X$ and $Y$ are positively related (a higher value of $X$ tends to correspond to a higher value of $Y$) then $\mathrm{cov}(X,Y) > 0$ and conversely if $X$ and $Y$ are negatively related then $\mathrm{cov}(X,Y) < 0$. If there is no relation between $X$ and $Y$ then $\mathrm{cov}(X,Y) = 0$. The value of the covariance however cannot be used as a determinate of correlation other than if it is 0, positive or negative. In order for the actual value to provide information on the strength of the correlation the covariance is divided by the standard deviation of $X$ and $Y$, $\sigma_X$ and $\sigma_Y$.

$$\rho = \frac{\mathrm{cov}(X,Y)}{\sigma_X \sigma_Y} \tag{4.3}$$

where $\rho$ is known as the correlation coefficient and the coefficient must be between 1 and -1.

For this experiment $X$ and $Y$ are the measurements from two different rounds of the same route and sensor. $x_i$ and $y_i$ are the individual measurements at a position $i$. The fast Fourier transform (FFT) is taken for both $X$ and $Y$:

$$X_{ft} = \mathrm{FFT}(X) \quad Y_{ft} = \mathrm{FTT}(Y) \tag{4.4}$$

Then the complex conjugate of $Y_{ft}$ ($Y_{ft}$*) is taken and the inverse fast Fourier transform (IFFT) of the product of $X_{ft}$ and $Y_{ft}$* gives the unnormalised cross correlation coefficient. Therefore so that autocorrelation at zero lag would be exactly one it is normalised by dividing by $\sigma_X$ and $\sigma_Y$. This then gives the normalised cross correlation coefficient ($\rho$)

$$\rho = \frac{\mathrm{IFFT}\left(X_{ft} Y_{ft}^*\right)}{\sigma_X \sigma_Y} \tag{4.5}$$

Here, the correlation coefficient is used to calculate the cross correlation of two rounds of sensor data. The correlation coefficient is a normalised value. If a signal is correlated with itself, at zero offset (autocorrelation) then this would give a value of 1, entirely uncorrelated data gives 0. Signals that are 180˚ out of phase would give a cross correlation value of -1.

### 4.2 Results

#### 4.2.1 Cross Correlation Coefficients

The cross correlation coefficients are shown in **Table 4** for all the sensors. It shows the coefficients for the four different road types using combinations of rounds (round 1 & 2, round 2 & 3 and round 1 & 3 for each three days) from the same days and the average of the coefficients for all the combinations. The sensors with higher coefficients are discussed in more detail in the following subsections. All sensors are discussed in detail in our *ION GNSS+ 2013* paper [14].

**Table 4 - Cross correlation coefficients for sensor outputs for the four road types**

| Sensor type | Cross Correlation Coefficient | | | |
|---|---|---|---|---|
| | High Speed | Rural | Urban | Suburban |
| Accelerometer | 0.00 | 0.01 | 0.03 | 0.01 |
| Air Quality | 0.33 | 0.26 | 0.09 | 0.16 |
| Barometer | 0.98 | 0.99 | 0.85 | 0.91 |
| Dust | -0.05 | -0.03 | 0.00 | 0.07 |
| Ambient Light | 0.31 | 0.59 | 0.31 | 0.77 |
| Magnetometer | 0.38 | 0.84 | 0.62 | 0.26 |
| Microphone | 0.53 | 0.59 | 0.39 | 0.17 |
| Thermometer | 0.29 | 0.52 | 0.10 | -0.05 |

NB. Roads signs does not have cross correlation coefficients calculated as this feature will be treated as discrete. Discrete features are discussed separately in Section 5.

### 4.2.2 Accelerometer

The magnitude of the acceleration from a accelerometer triad was used in this experiment as a method of measuring road texture and also vehicle movement. A zoomed in section of the acceleration as recorded from the accelerometer against the distance travelled can be seen in **Figure 7**.

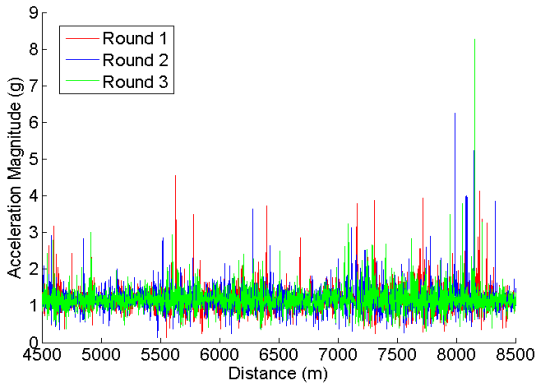


**Figure 7 -** Profile from accelerometer (ADXL345) attached to axle

It is difficult to see similarities in the output from the different rounds although the accelerometer can show movement from stationary to driving and this was used to initialise the sensor outputs from the XSens IMU. This is shown in **Figure 8** at 44s.

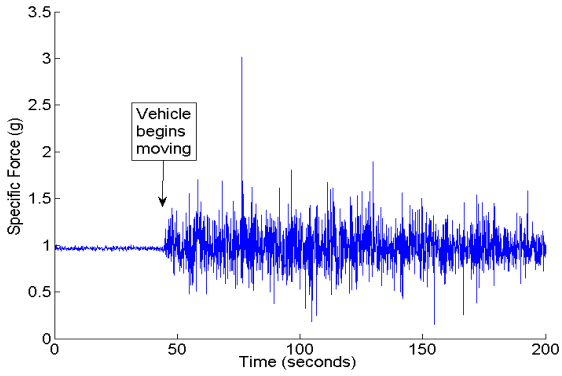


**Figure 8 -** Accelerometer data showing vehicle setting off

### 4.2.3 Barometer

The barometer is used to measure the height change of the vehicle. This sensor produced consistently the highest cross correlation coefficient. This can be seen in **Figure 9**.

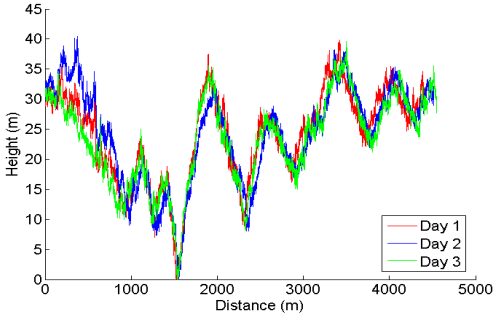


**Figure 9 -** Comparison of height profile over 3 days with minimums set to zero

### 4.2.4 Magnetometer

The magnetometer produced data with distinct spikes caused by various magnetic anomalies in the environment being travelled through this can be seen in **Figure 10** for the high speed road.

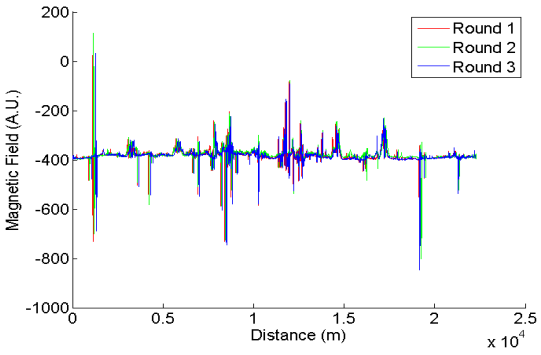


**Figure 10** – Vertical axis magnetic field profile for a high speed road

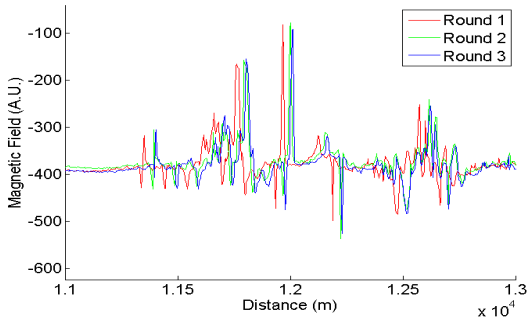


**Figure 11 -** Zoomed in section of the vertical axis magnetic field experienced on a high speed road

**Figure 11** is a zoomed in section of the magnetometer data from the high speed road in **Figure 10**. It shows correlation with an offset of approximately 44m between round 1 and round 3. This is mostly due to synchronisation errors between the magnetometer counter and the GNSS receiver clock. This is the reason a second run of the road experiment was completed and this was discussed at the end of section 0.

### 4.2.5 Microphone

The microphone was able to pick up clear signals when the vehicle was stationary and the signal seems to be dependent on the speed of the vehicle. **Figure 12** shows the profile from the microphone.

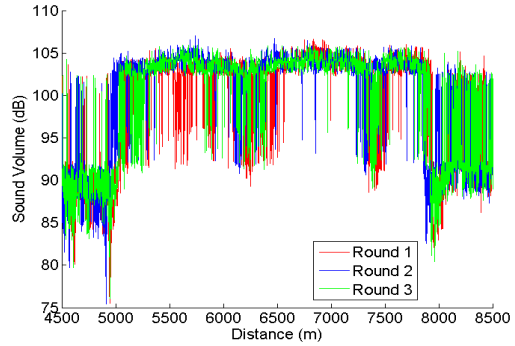


**Figure 12 -** Profile from microphone attached to axle

It may be possible to combine this data with the accelerometer or odometer data to develop a clearer picture of what sound is resulting directly from the road surface and what is speed related, although this still may not result in a useful feature for this study.

### 4.2.6 Thermometer

Temperature can be seen to vary particularly in a rural environment as can be seen in **Figure 13**.

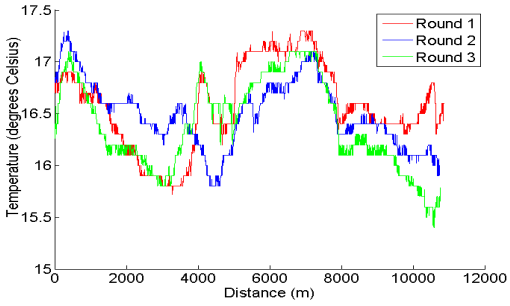


**Figure 13** - Temperature profile for rural roads

The similarities though are not consistent across environments as can be seen from the cross correlation values in **Table 4** and are likely to change with the seasons and due to weather conditions.

### 4.2.7 Light Sensor

Four light sensors were used in the experiment: upwards, forwards, left and right facing. **Figure 14** shows the data from the upward facing sensor on the high speed road. There are distinct events where the light level drops. In these instances many correspond to gantries (bridge like structure spanning highways displaying speed limits and other information). These features could be treated as discrete, whereby the sharp dips in light level would be treated as momentary events. Some of the information would be lost in treating the ambient light as discrete but it would make the feature more robust against changing light levels due to shadowing or cloud cover.

If light is treated as a continuous feature it can be seen in **Table 4** that the cross correlation was inconsistent. This is partly due to the effects of changing light conditions. On the days with direct sunlight, the light sensor would reach its maximum intensity and be saturated. This can be seen in **Figure 14** and this affects the cross correlation coefficient calculated.

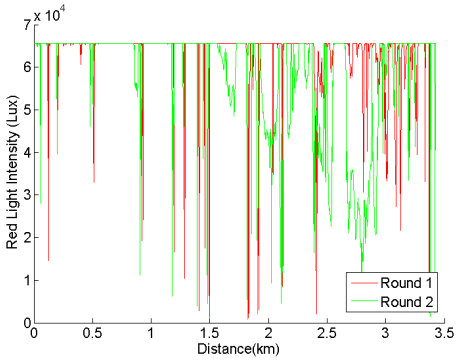


**Figure 14** – The upward-facing light sensor profile for the high speed road in second experiment day two

### 4.3 Feature outcome

The thermometer data has been discounted as although it gave a cross correlation coefficient of about 0.5 for the rural route the other routes had lower cross correlation values. Similarly, the microphone data had moderate

success in high speed and rural environments but not in the other two routes. Therefore it will not be taken forward to the next phase although it could be used in the future if further processing was carried out on the data. As with the microphone, the light sensor had cross correlation values greater than 0.5 in the rural and urban environments but had lower values in the other two. The success of this sensor is more reliant on the weather conditions than the environment type. At the current point this will not be brought forward to the next stage

The accelerometer (used to measure road texture) showed no correlation with cross correlation coefficients of approximately zero (between 0.0 and 0.3). It was useful for use in dead reckoning but does not illustrate road texture.

The magnetometer and barometer showed the greatest potential for positioning with the highest cross correlation values consistently over all the environments. These sensors are taken forward into phase 3.

Road signs will be discussed in detail in the next section which illustrates a method of measuring the similarities of a sequence of discrete events.

## 5. PHASE 2 FOR DISCRETE FEATURES

A discrete feature is one where there are environmental events which occur at one position but can repeat multiple times along a route. The discrete feature can either be Boolean (an event occurs or does not) or it can be descriptive (different possible events or the strength of the event). Examples of discrete features include lamp-posts, speed humps and shop signage.

In this paper the discrete feature that will be discussed will be street signs although the techniques used are applicable to many discrete features. How the signs are identified will also not be discussed in detail in this paper and instead focus will be on how a sequence of discrete features is used show consistency across a route.

As an overview the signs were identified manually. This is a temporary measure and it is hoped that future work will automate the process. The manual process involved noting the type of sign and the time they were seen. The time-stamp was taken at the first point at which the sign could be discernible.

When the technique is automated, considerations will need to be made for when to state the signs is seen, the solution likely to provide the highest consistency is if the time is taken once the identified sign is a specific size in the footage. This then gives a determinable range to that sign and as the British traffic signs are a particular size then this would mean the actual position could be calculated. Once all the signs along a route were recorded it was important to find a method which could use a sequence of signs to determine quantitatively how similar that sequence is to that of the sign recorded on a different round. As with the continuous data the first step is to compare the full rounds data with a different round's data. The next subsection will describe the method used to quantify how similar two sign sequences are and how it is used with the road experiment's data.

### 5.1 Damerau-Levenshtein Distance

Damerau-Levenshtein Distance (DLD) [22] [23] is a method of comparing a sequence for discrete events (or strings). It measures the minimum number of changes needed to convert one string into another. If each sign is assigned a letter this would produce a string that can be analysed using DLD. The changes allowed with the DLD method are substitution, addition, deletion and transposition. In the conventional DLD technique every change type is assigned a value of one. Once all changes are made to the second string to become the first string the total DLD score is tallied. The more changes needed the higher the score will be in traditional DLD. If the two strings are identical then the DLD score will be zero and if the strings are completely different the score is the number of characters in the longer string.

In order for DLD technique to give a comparable value to the cross correlation coefficients used for continuous features, two additional steps were added to augment the conventional technique.

$$D_{score} = \left(1 - \frac{D_{DLD}}{n}\right) \tag{5.1}$$

Equation 5.1 shows the two additional steps added to the traditional DLD method to create the DLD-augmented scores ($D_{score}$) used in this paper.

The first step is to ensure that all DLD score values are between 0 and 1. To do this the DLD score ($D_{DLD}$) is divided by the length of the longest string ($n$). This is because this is largest number of changes that is needed to produce identical strings. Then to normalise the DLD score so 1 means that the strings are identical and 0 means the strings are completely dissimilar.

A worked example can be seen in **Table 5**. The example uses two strings: Walters and Wantler.

**Table 5- DLD word example**

| **W** | **A** | | **L** | **T** | **E** | **R** | **S** |
|---|---|---|---|---|---|---|---|
| • | • | + | ↔ | ↔ | • | • | - |
| **W** | **A** | **N** | **T** | **L** | **E** | **R** | |

where • is no change, ↔ is transposition, + is addition and - is deletion.

$$\begin{aligned} D_{score} &= \left(1 - \frac{D_{DLD}}{n}\right) \\ &= \left(1 - \frac{3}{7}\right) \\ &= 0.57 \end{aligned} \tag{5.2}$$

Equation 5.2 shows for the two strings Walters and Wantler that $D_{score}$ is 0.57.

### 5.2 Road sign results using DLD

British road traffic signs (many of which are international) were placed into six categories and these categories can be seen in **Table 6**.

**Table 6 - Categories of signs detected with ID and example**

| Sign ID | Sign Description | Example |
|---|---|---|
| 1 | Red outlined circular signs | Speed limit sign |
| 2 | Red outlined triangular signs | Crossroads ahead sign |
| 3 | Blue signs with white arrow | One way sign |
| 4 | Green rectangular signs | A road information sign |
| 5 | Brown rectangular signs | Tourist information sign |
| 6 | Blue rectangular without arrows | Motorway information sign |

To illustrate this method all of the signs observed along a selection of full routes were analysed to calculate $D_{score}$. The outcome from suburban and urban environments can be seen in **Table 7.**

**Table 7 - $D_{score}$ for roads signs on combinations of rounds on suburban and urban routes, including average and Standard Deviation (SD) of $D_{score}$**

| 1st Round | 2nd Round | Suburban $D_{score}$ |
|---|---|---|
| D2 R2 | D2 R3 | 0.58 |
| D2 R2 | D3 R1 | 0.62 |
| D2 R2 | D3 R2 | 0.56 |
| D2 R3 | D3 R1 | 0.33 |
| D2 R3 | D3 R2 | 0.56 |
| D3 R1 | D3 R2 | 0.84 |
| Average | | 0.58 |
| SD | | 0.16 |

| 1st Round | 2nd Round | Urban $D_{score}$ |
|---|---|---|
| D2 R1 | D2 R3 | 0.85 |
| D2 R1 | D3 R1 | 0.55 |
| D2 R1 | D3 R2 | 0.43 |
| D2 R3 | D3 R1 | 0.55 |
| D2 R3 | D3 R2 | 0.57 |
| D3 R1 | D3 R2 | 0.74 |
| Average | | 0.62 |
| SD | | 0.15 |

The days and rounds are shown as D*X* R*X* where D is day and R is round. If $D_{score}$ is close to 1 that means that the signs seen along the full route are similar. The lower the number the more dissimilar the sequence of signs seen along the route are. Also analysis was carried out on how well DLD could distinguish the same road environment with different road environments. On average a $D_{score}$ of 0.66 was found when comparing rounds for the same route whereas comparing rounds from different routes the average $D_{score}$ was 0.2. This shows that this method can determine if the route is same or different using the test data from the road experiment.

Therefore the augmented DLD method gives a comparable method of comparing discrete feature's matching success to that of continuous features.

## 6. PHASE 3 – REGION IDENTIFICATION

### 6.1 Region Identification Technique

As the magnetometer and barometer had the highest cross correlation values these features will be used in phase 3. Road signs have also been brought through to phase 3 but will be dealt with slightly differently and was discussed in Section 5. This section will cover a technique used to match regions selected from road environments with the same regions from a different time or day. The aim of this is to determine if regions contain sufficient information to be differentiable from other regions in the same environment and also if there is repeatability when measurements are taken at different times. The data from the road experiment described in Section 3 is used for this analysis.

A region matching technique was devised to determine if there was sufficient information from the road experiment data to correctly identify a selected region along a route on a particular round is the same region from a different round. This was accomplished by taking data (from the magnetometer and barometer) from a number of regions along the route and comparing these with the data from the same regions on different rounds. **Figure 15** shows an example of comparing four regions over two rounds. Regions A, B, C and D are cross correlated with regions a, b, c and d. Hypothetical sensor data and their comparisons can be seen in **Figure 16**; the arrows show which of the capital letter regions is matched to lower case letter regions. In that example the matching success rate is 75%.

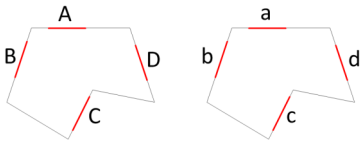


**Figure 15 -** Example of regions along a route. The regions from the two rounds are highlighted in red.

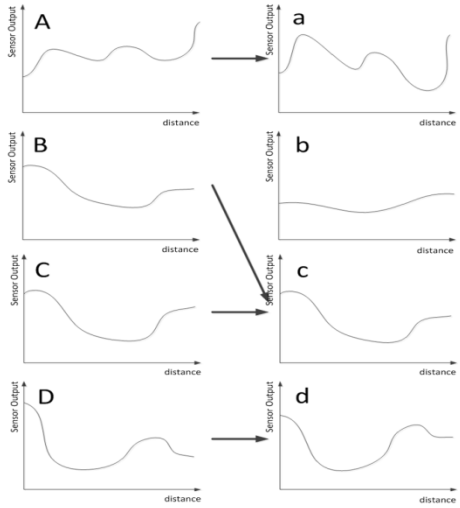


**Figure 16 -** Hypothetical traces from a sensor along a route for two rounds. Arrows show which rounds are matched.

In order to decide which of the regions are likely to be the matching region a table of cross correlation coefficients will be produced**. Table 8** shows the format of the cross correlation table.

**Table 8 - Example cross correlation table, red shows incorrect match and green correct**

| | | Round1 | | | |
|---|---|---|---|---|---|
| | | Reg1 | Reg2 | Reg3 | Reg4 |
| Round 2 | Reg1 | *Aa* | *Ba* | *Ca* | *Da* |
| | Reg2 | *Ab* | *Bb* | *Cb* | *Db* |
| | Reg3 | *Ac* | *Bc* | *Cc* | *Dc* |
| | Reg4 | *Ad* | *Bd* | *Cd* | *Dd* |

For example, the top left cell is the cross correlation coefficient for the first region (A) from round 1 with the first region (a) from round 2. The neighbouring cell to the left is the coefficient for the second region (B) for round one with the first region (a) from round 2. The table has in total 16 elements for all the combinations of regions over the two rounds. The highest value in each column represents the most likely match for the two rounds. Therefore for the regions to be correctly matched the diagonal elements (Aa, Bb, Cc, Dd) should produce the values closest one. In green and red are the results of the hypothetical example in Figure 16. Green is a correct match and red is an incorrect match.

### 6.2 Results

For this paper regional analysis is shown for suburban data taking the data from the 1st and 2nd round on the 3rd day of the road experiment. The full traces for magnetic and height can be seen in **Figure 17** and **Figure 18** respectively.

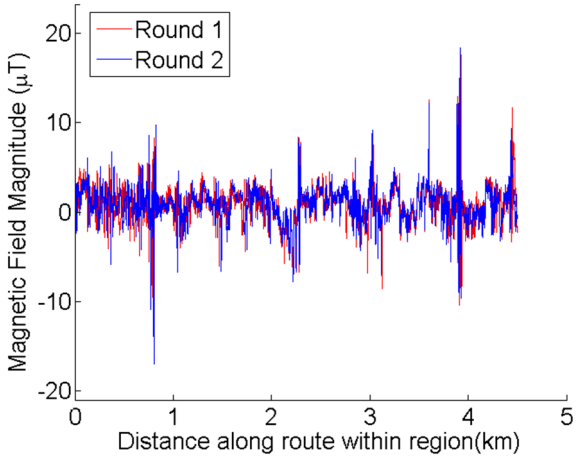


**Figure 17 -** The signal from the magnetometer for the full route for rounds 1 and 2 on day 3 in a suburban

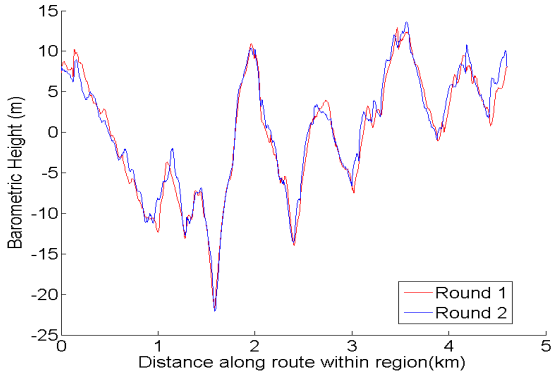


**Figure 18 -** The signal from the barometer for the full route for rounds 1 and 2 on day 3 in a suburban

The number of regions to be used was chosen as this impacts the probability of chance matching. 10 regions means that by random chance alone there is 10% chance of matching. Ten regions for an approximately 5km circuit were chosen as a balance between number of regions needed to reduce chance and also allow sufficient region lengths. The resulting 10 regions can be seen in **Figure 19.** Blue is used to highlight the regions and the arrows show the direction of travel in these regions. Each region was 200m long and the height data was smoothed using a moving average with a span of 99m.

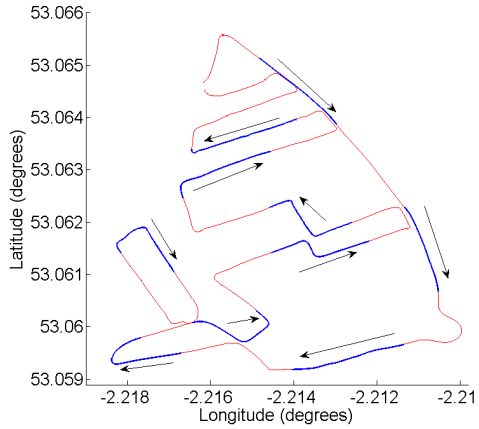


**Figure 19 -** Location of the 10 blue regions along the suburban route

The 10 by 10 cross correlation table for the suburban road magnetic data can be seen in **Table 9.** The highlighted text is the highest correlation coefficient per column. If the highest correlation coefficient per column corresponds to the correct region this is considered a successful match (green). Red signifies an incorrect match. For this ten region magnetic field data there was a 90% matching success.

**Table 9 - Table showing correlation coefficients from 10 regions within the suburban route using magnetometer data -**

| Magnetic Field | | Round1 | | | | | | | | | |
|---|---|---|---|---|---|---|---|---|---|---|---|
| | | Reg1 | Reg2 | Reg3 | Reg4 | Reg5 | Reg6 | Reg7 | Reg8 | Reg9 | Reg10 |
| Round 2 | Reg1 | 0.62 | 0.36 | 0.30 | 0.27 | 0.22 | 0.22 | 0.37 | 0.21 | 0.28 | 0.25 |
| | Reg2 | 0.38 | 0.81 | 0.34 | 0.32 | 0.34 | 0.34 | 0.24 | 0.15 | 0.26 | 0.36 |
| | Reg3 | 0.26 | 0.33 | 0.56 | 0.59 | 0.19 | 0.43 | 0.38 | 0.47 | 0.31 | 0.25 |
| | Reg4 | 0.21 | 0.32 | 0.46 | 0.77 | 0.31 | 0.36 | 0.27 | 0.31 | 0.23 | 0.32 |
| | Reg5 | 0.26 | 0.30 | 0.31 | 0.27 | 0.57 | 0.33 | 0.39 | 0.25 | 0.41 | 0.33 |
| | Reg6 | 0.24 | 0.37 | 0.41 | 0.39 | 0.22 | 0.76 | 0.30 | 0.38 | 0.23 | 0.43 |
| | Reg7 | 0.24 | 0.35 | 0.30 | 0.21 | 0.32 | 0.28 | 0.67 | 0.29 | 0.39 | 0.25 |
| | Reg8 | 0.18 | 0.36 | 0.48 | 0.40 | 0.39 | 0.38 | 0.32 | 0.91 | 0.41 | 0.21 |
| | Reg9 | 0.21 | 0.25 | 0.19 | 0.27 | 0.36 | 0.27 | 0.48 | 0.38 | 0.80 | 0.25 |
| | Reg10 | 0.27 | 0.24 | 0.24 | 0.42 | 0.35 | 0.35 | 0.22 | 0.23 | 0.29 | 0.42 |

**Table 10 - Table showing correlation coefficients from 10 regions within the suburban route using barometer data**

| Barometric Height | | Round 1 | | | | | | | | | |
|---|---|---|---|---|---|---|---|---|---|---|---|
| | | Reg1 | Reg2 | Reg3 | Reg4 | Reg5 | Reg6 | Reg7 | Reg8 | Reg9 | Reg10 |
| Round 2 | Reg1 | 0.69 | 0.93 | 0.57 | 0.50 | 0.69 | 0.43 | 0.96 | 0.52 | 0.97 | 0.43 |
| | Reg2 | 0.86 | 0.93 | 0.36 | 0.42 | 0.66 | 0.52 | 0.92 | 0.43 | 0.97 | 0.45 |
| | Reg3 | 0.71 | 0.87 | 0.62 | 0.71 | 0.89 | 0.51 | 0.87 | 0.47 | 0.80 | 0.44 |
| | Reg4 | 0.64 | 0.49 | 0.75 | 0.97 | 0.74 | 0.61 | 0.53 | 0.50 | 0.45 | 0.40 |
| | Reg5 | 0.85 | 0.72 | 0.80 | 0.79 | 0.96 | 0.54 | 0.70 | 0.37 | 0.64 | 0.41 |
| | Reg6 | 0.65 | 0.48 | 0.68 | 0.77 | 0.66 | 0.87 | 0.54 | 0.36 | 0.48 | 0.60 |
| | Reg7 | 0.70 | 0.97 | 0.55 | 0.54 | 0.72 | 0.44 | 0.98 | 0.51 | 0.97 | 0.47 |
| | Reg8 | 0.43 | 0.42 | 0.48 | 0.45 | 0.42 | 0.87 | 0.36 | 0.69 | 0.46 | 0.58 |
| | Reg9 | 0.80 | 0.97 | 0.46 | 0.45 | 0.65 | 0.48 | 0.97 | 0.46 | 0.98 | 0.48 |
| | Reg10 | 0.59 | 0.53 | 0.46 | 0.42 | 0.57 | 0.59 | 0.51 | 0.78 | 0.49 | 0.70 |

The same analysis was carried out for the height data and the resulting matrix can be seen in **Table 10.** The height data matched the correct region 40% of the time. This may mean that for a region size of 200m the height cannot provide the required accuracy and a larger region size maybe useful for this particular feature. It should be noted though that if the terrain is too flat increasing region length would not improve the matching success.

### 6.2.1 Region Length

The length of the regions is one of the fundamental considerations that needs to be decided upon. This section investigates the effect it has on the success of matching the regions. **Figure 20** shows the matching success against region size for the 4 different road types. Ten regions were used in this analysis with results for different regions lengths and road types shown. The region lengths ranged from 20m to 1500m and there were three runs of the analysis using ten different regions each time. The locations of the ten regions used were equally spread over the full route and in order to run the analysis three times the ten regions were shifted by 50m on the 2nd run and 100m for the 3rd run. Therefore different sections of the route were analysed each time. For this figure magnetic and height data have been combined with equal weighting. More analysis on weighting is found in Section 8.

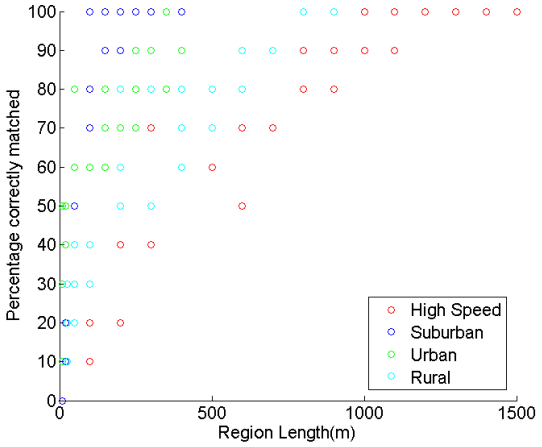


**Figure 20** -Matching success vs region length for all four road types

From **Figure 20**, it can be seen that suburban and urban data generally achieves matching success at smaller region sizes than is required for the rural and high speed data. The vehicle during the suburban and urban experiment was travelling at a slower average speed than in the other two road types and this would mean that there are a greater number of data points for a given distance (assuming that the sensor can detect variations in the feature faster than the sample rate used in the experiment).

To achieve 90%/70% success rate the minimum region length to achieve this success was taken from the data in **Figure 20**. This is shown in **Table 11** and shows clearly that the higher speed roads need far higher region sizes than the slower roads (suburban and urban) to achieve the same success.

**Table 11 – Minimum region size to achieve 90% and 75% region matching success based on Figure 20**

| Road Type | High Speed | Suburban | Rural | Urban |
|---|---|---|---|---|
| 90% success | 700m | 100m | 600m | 140m |
| 70% success | 300m | 100m | 200m | 60m |

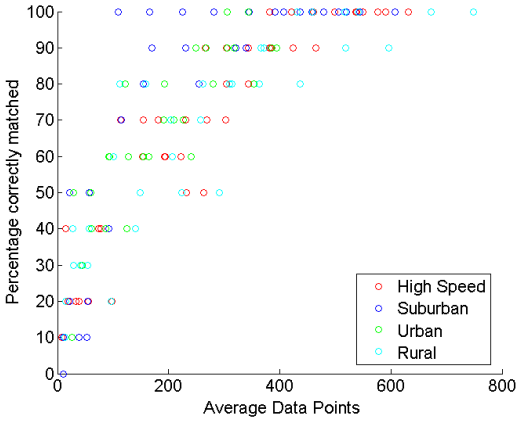


**Figure 21** - Matching success of regions vs number of data points for the region for all four road types

To verify if this hypothesis is true (that greater number of data points improves matching success) a second figure was produced showing this time the number of data points that are in a region against matching success. In **Figure 21** there is still a spread of results but the different road types no longer appear as clearly banded areas on the graph. This suggests that the amount of data points has a significant effect on the ability for the regions to be correctly matched (although this is unlikely to be the sole effect on the measurements). Therefore it is important to determine the optimal sampling rate; too low means useful information will be discarded and too high and processing resource will be wasted.

## 7. PHASE 4 – POSITION DETERMINATION: SCANNING METHOD

### 7.1 Method

The previous section has used set regions and compared these same regions over different rounds to determine which match. This section will look at scanning one round to find the region which best matches a region from a different round. **Figure 22** illustrates this technique.

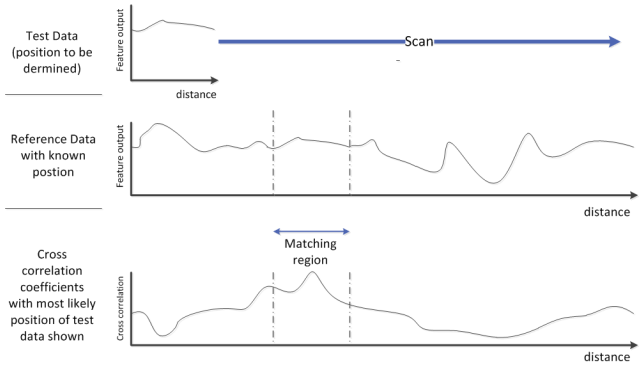


**Figure 22**- Diagram showing the principle used to scan for best match to a pre-set region

The test data is scanned through the reference data. Cross correlation coefficients are calculated as the test data is scanned through. The aim is to locate the position of the test data using the reference data for which the position is already known. The output of this exercise gives a cross correlation profile (cross correlation as a function of position). This profile can be treated similarly to a probability density distribution of position (although they are not the same) and so gives an idea of the probability of the position at each point in the test data.

### 7.2 Results

Two rounds from the suburban route are shown in this section as an example of the results achieved with the scanning method. **Figure 23** and **Figure 24** show the cross correlation profiles for magnetic field and height for day 3 rounds 1 and 2 on the suburban route respectively. The test data region chosen is centred at 1.6km into the route. The test data region size was 125m for 4.5km reference data.

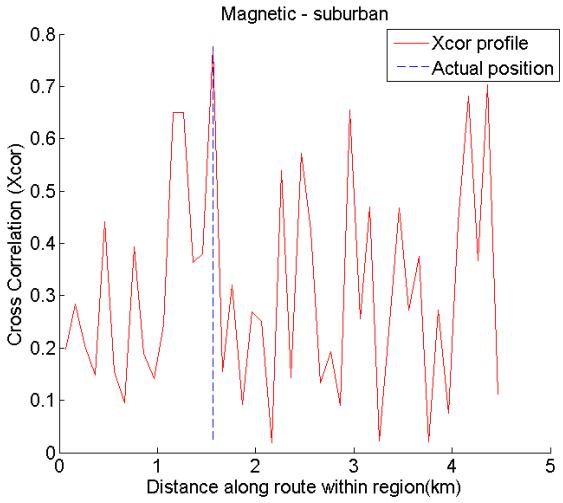


**Figure 23** - Cross correlation scan for magnetic field on the suburban route with the centre of the actual position of the test data shown as blue dotted line

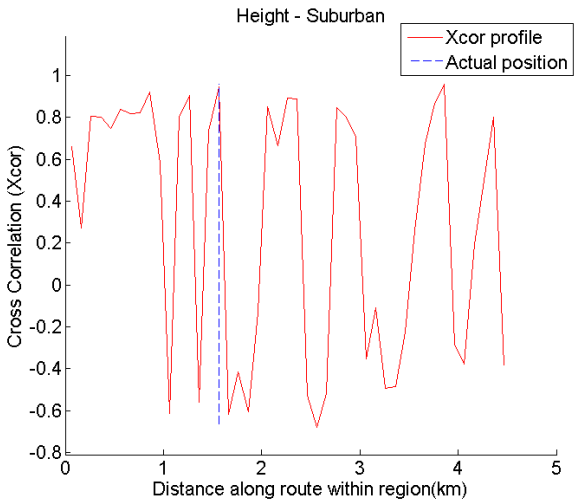


**Figure 24** - Cross correlation scan for the barometric height on the suburban route with the centre of the actual position shown as blue dotted line

It can be seen that the magnetic field has a number of peaks along the route. The peak with the highest cross correlation coefficient is at the 1.6km point (which is the correct position). For the height figure there are many broad peaks at similar cross correlation values approximately 700m apart. The height peaks are broader than the magnetic peaks because the terrain height changes more slowly than the magnetic field.

### 7.2.1 Ambiguities and dead reckoning

The two graphs in **Figure 23** and **Figure 24** show that there are ambiguities present in both of the features. The majority of the features will have some ambiguities along a route and so it is important to develop a technique that could mitigate them. One way ambiguities could be mitigated is by using the information available from dead reckoning. The dead reckoning solution will have a specific position error (which grows with time) and the ambiguities from the features can be reduced by only considering the candidate position within the dead reckoning position uncertainty bounds. Equations 7.1 and 7.2 show the standard deviation which can be used to calculate the uncertainty bounds for the position.

$$\mathbf{r}_k = \mathbf{r}_{k-1} + \Delta\mathbf{r}_k \quad (7.1)$$

$$\sigma^2_{\mathbf{r}_k} = \sigma^2_{\mathbf{r}_{k-1}} + \sigma^2_{\Delta\mathbf{r}_k} \quad (7.2)$$

Where σ is standard deviation, $\mathbf{r}_{k-1}$ is last known position fix, $\mathbf{r}_k$ is the current position and $\Delta\mathbf{r}_k$ is the change in position using dead reckoning.

The search region therefore could be limited to within 3 standard deviations of the dead reckoning which is equivalent to a 99.73% confidence interval. An additional benefit of using the dead reckoning standard deviation is that it reduces computational load as cross correlation values will only need to be calculated within that range.

## 8. PHASE 5 – COMBINATION OF FEATURES

The quality of position information that can be extracted from a particular feature type varies with location. Thus a better position solution can be obtained if higher weighting is attributed to higher quality features. Factors that will need to be considered include the precision of position that can be extracted from a feature, the level of ambiguity (are there multiple candidate positions) [9] and the reliability (how much measurements vary unpredictably with time).

In Sections 4.2.1and 5.2 methods of measuring scoring for continuous and discrete features were discussed. The next step was to find an optimal method of combining these scores($D_{score}$ or $\rho$). Section 6.2.1 showed the combination of magnetic field and barometric height cross correlations using equal weighting. This section will look at other possible combinations of weightings.

### 8.1 Possible combination techniques

There are multiple ways to combine the scores from different features. Initially there is the decision as to when in the position estimation process to combine the features. There are two ways to do this either combine the scores for each feature or combine the position estimates for each sensor. The following subsections will describe a number of ways of combining the scores before estimating the position. It will be noted if these techniques could also be used to combine position estimates.

### 8.1.1 Equal weighting

A simple combination technique is for each feature score to have equal weighting. The equal weighting used in Section 6.2.1 took the two scores and found the average. This way no single feature will dominate the navigation solution. As the feature scores are not probabilities the values are not self-weighting therefore it cannot be presumed that that equal weighting would always provide an optimal position estimation.

### 8.1.2 Test data weighting

This method takes a set of experimental data and empirically determines the weighting coefficients based on the best position solution in this test dataset. The test data would be used to maximise the score of the combined features using weighting at the correct position. This would have the benefit of using real data to determine the weighting but its strength is based on how representative the test dataset is to the environments that the car will travel in.

### 8.1.3 Environmental context-dependent weighting

This method would detect the environmental context and use this to select an appropriate set of weights. [24] [9]. For example, the presence of many Wi-Fi sources would suggest a suburban or urban environment while a vehicle speed of 31m/s (70mph/113km/h) would suggest that the vehicle is likely to be on a highway. Based on this knowledge it would possible to use a specific weighting coefficient set that is developed for that environmental context.

### 8.1.4 Cross correlation profile weighting

This method weights each feature according to the characteristics of the cross correlation coefficients profile obtained using the scanning method described in Section 7. This enables the weighing to adapt to the quality of the data. **Figure 25** shows the traits of a set of peaks that affect the confidence in the highest peak being the correct position.

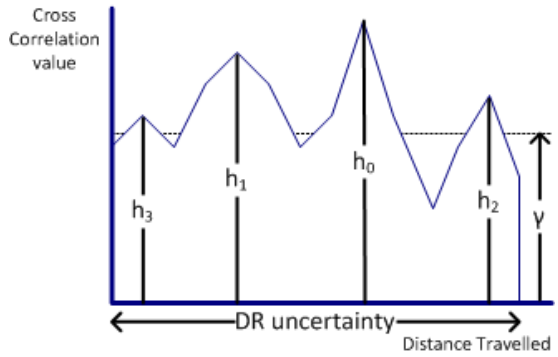


**Figure 25 -** Weighting nomenclature

Taking the uncertainty in the current position (as shown in equation 7.2 in Section 7.2.1) only peaks that, for example, fall within 3 standard deviations ($3\sigma$) would be evaluated. The characteristics of the tallest peaks compared with the others would be used to determine a measure of confidence for that feature.

There will be more confidence in the tallest peak ($h_0$) if there is a greater difference between its height and that of the other peaks within the uncertainty range ($h_{1,2,3}$), In **Table 12** this is Δ Height..

The next factor is the number of peaks within the uncertainty range (No. Peaks). The more peaks the less confidence there is that the correct peak has been chosen as the position estimate.

The average cross correlation coefficient within the uncertainty region ($\gamma$) would affect the confidence in the estimated position. If the average coefficient value (Av. CC) was similar to that of the highest peak, this would suggest there is insufficient variation in the data being analysed from that feature.

Finally the standard deviation could be used. By calculating how many standard deviation (Std Dev) the highest peak was from the mean this could provide a weighting value.

Each of these characteristics was looked at separately and compared against the benchmark of equal weighting using the scanning method comparing multiple pairs of rounds on different routes. It can be seen in **Table 12** that the standard deviation from the mean provided the best weighting outcomes. To optimise the weighting algorithm it may be that using a combination of these profile characteristics would provide the best position estimation.

**Table 12 - Cross correlation profile weighting showing the average distance from the true position of the vehicle and the percentage of times the weighted scanning technique calculated the position within 100m**

| | Equal | Δ Height | No. Peaks | Av. CC | Std Dev |
|---|---|---|---|---|---|
| Distance from Truth | 86m | 87m | 94m | 101m | 82m |
| % within 100m | 63% | 62% | 60% | 55% | 66% |

**Figure 26** and **Figure 27** show examples of cross correlation profiles, they show high and low confidence respectively. **Figure 26** is the cross correlation of data from day three, rounds two and three on suburban roads. This figure has a few spaced out peak over the full profile and one of the peaks is clearly higher than the others. **Figure 27** is the cross correlation of data from day two, round three and day three, round three from the high speed road. This figure has many similar height peaks all around the value of 0.5.

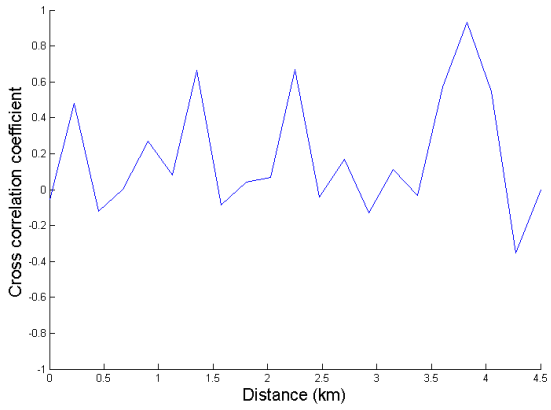


**Figure 26** - Good cross correlation profile; few spaced out peaks with one higher than all other peaks

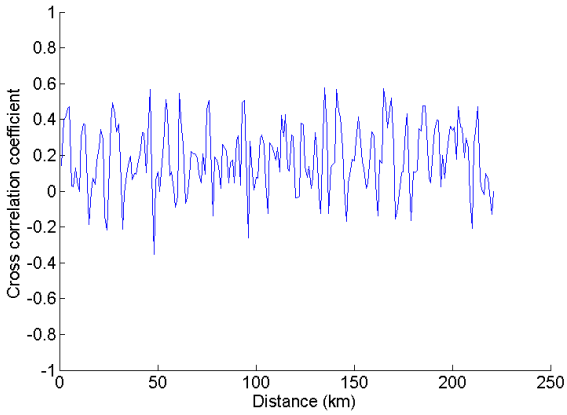


**Figure 27 -** Poor cross correlation profile; many low similar height peaks

## 9. CONCLUSION

This paper presents the results of a five part feasibility study into the use of environmental features as a basis for predicting the location of a body as it navigates through the environment.

The literature-based element highlighted features such as magnetic field anomalies, ambient light, road texture and terrain height as possible features to bring forward into the next stage of the study.

A road experiment was described which collected data that was used in the rest of the paper. The second phase of the feasibility study showed that multiple sensors could be used to provide consistent measurements when the same route is repeated over multiple trips and days. Initially cross correlation coefficients were calculated over full routes. Promise was seen in particular in the magnetic field and barometric height data collected.

For environmental features that occur at discrete events, such as road signs, a different technique was used. A modified Damerau-Levenshtein Distance was developed that takes a sequence of recently observed signs and compares this with the sequence of signs from previously collected data. The method can produce similar scores to the cross correlation coefficients from the other environmental features and produced a three times higher score for comparing same routes than different routes.

The third stage of the feasibility study showed that by splitting a route into regions it is possible to locate which regions are the same from a selection of regions taken from different rounds. This means there is sufficient variation in features in the environment and that they remain reasonably static and repeatable. This demonstrates that the sensors provide sufficient information to use them for positioning.

The fourth stage of the feasibility study delivered a scanning method which provides an estimated position for the vehicle. The scanning method takes a selection of recently collected data and scans the database to determine where in the database these measurements are likely to correspond to.

The fifth and final stage of the feasibility study discussed a selection of methods of weighting including equal weighting which was used in stage three as well as a method to use the characteristics of cross correlation coefficient profile produced from the scanning method. Using a method using the number of standard deviations the cross correlation peak is from the mean there is an improvement in position estimation of 4m.

This study has shown that environmental features have sufficient variability spatially and stability temporally for a database of features to be developed to create a map of the environment. These results support the hypothesis that it is feasible to map a space and then go forward to create a feature-mapping and navigation algorithm using a combination of environmental feature sensors, a GNSS receiver and sensors for dead reckoning.

## 10. FUTURE WORK

The next step of the project is to develop a feature-matching, mapping and navigation algorithm which incorporates inputs from the multiple sensors, a GNSS receiver, map-matching and sensors for dead reckoning. The algorithm will run collecting sensor data while GNSS receiver data is available and store this in a database along with location stamps until called upon in times of GNSS receiver signal disturbance. The data from the road experiments will be used for a test database in developing the navigation system.

## ACKNOWLEDGEMENTS

Debbie Walter is jointly funded by Engineering and Physical Sciences Research Council (EPSRC) and Terrafix ltd.

The authors would like to thank Paul Neesham for developing a method of manually recording street signs seen in video footage and Juliusz Romaniuk of Terrafix for his advice and for creating the hardware unit attached to the vehicle in the road experiment which contained the sensors.

## REFERENCES

[1] Royal Academy of Engineering, “Global Navigation Space Systems: Reliance and Vulnerabilities,” March 2011.

[2] P. D. Groves, Principles of GNSS, Inertial and Multisensor Integrated Navigation Systems, 2nd ed., Artech House, 2013.

[3] C. Hide, T. Moore, C. Hill, C. Noakes and D. Park, “Integrated GPD, LORAN-C and INS for Land Navigation Applications,” in *ION GNSS*, 2006.

[4] T. Webb, P. Groves, P. Cross, R. Mason and J. Harrison, “A New Differential Positioning Method Using Modulation Correlation of Signals of Opportunity,” in *IEEE/ION PLANS*, Indian Wells, CA , 2010.

[5] T. A. Webb, P. D. Groves, R. J. Mason and J. H. Harrison, “A New Differential Positioning Technique Applicable to Generic FDMA Signals of Opportunity,"," in *24th International ION GNSS+*, 2011..

[6] D. Palmer, T. Moore, C. Hill, M. Andreotti and D. Park, “Radio Positioning using the Digital Audio Broadcasting (DAB) Signal,” *The Journal of Navigation,* vol. 64, no. 1, pp. 45-59, 2011.

[7] W. Churchill and P. Newman, “Continually Improving Large Scale Long Term Visual Navigation of a Vehicle in Dynamic Urban Environments,” in *IEE Intelligent Transportation Systems Conference*, 2012.

[8] M. J. Veth, "Navigation Using Images, A Survey of Techniques," *NAVIGATION, Journal of the Institute of Navigation, ,* vol. 58, no. 2, pp. 127 - 139, 2011.

[9] P. Groves, L. Wang, D. Walter, H. Martin, K. Voutsis and Z. Jiang, "The Four Key Challenges of Advanced Multisensor Navigation and Positioning," in *IEEE/ION PLANS*, Monterey, California, 2014.

[10] P. D. Groves, "The Complexity Problem in Future Multisensor Navigation and Positioning Systems: A Modular Solution," *Journal of Navigation,* vol. 67, no. 3, 2014.

[11] P. Groves, H. Martin, K. Voutsis, D. Walter and L. Wang, "Context Detection, Categorization and Connectivity for Advanced Adaptive Integrated Navigation," in *ION GNSS+*, Nashville, TN, 2013.

[12] M. Adjrad and P. D. Groves, "Enhancing Conventional GNSS Positioning with 3D Mapping without Accurate Prior Knowledge," in *ION GNSS+*, Tampa, FL., 2015.

[13] P. Groves, M. Adjrad, L. Wang and C. Ellul, "GNSS Shadow Matching: The Challenges Ahead," in *ION GNSS+* , Tampa, FL., 2015.

[14] D. Walter, P. D. Groves, B. Mason, J. Harrison, J. Woodward and P. Wright, "Novel Environmental Features for Robust Multisensor Navigation," in *ION GNSS+*, 2013.

[15] Y. L. a. X. L. Andrzej Ruta, "Real-time traffic sign recognition from video by class-specific discriminative features," *Pattern Recognition,* no. 43, pp. 416-430, 2010.

[16] Gov.uk, "Traffic Signs," [Online]. Available: https://www.gov.uk/traffic-signs. [Accessed 2013 August].

[17] G. Wyszecki and W. S. Stiles, Color Science: Concepts and Methods, Quantitative Data and Formulae, 2nd, Ed., Wiley, 2013.

[18] J. Shockley and J. Racquet, "Navigation of Ground Vehicles using Magnetic Field Variations," *NAVIGATION,* vol. 4, no. 4, pp. 237-252, 2014.

[19] W. Soehren and W. Hawkinson, "A Prototype Personal Navigation System," in *IEEE/ION PLANS*, 2006.

[20] T. Sönmez and H. E. Bingöl, "Modeling and Simulation of a Terrain Aided Inertial Navigation Algorithm for Land Vehicles," in *IEEE/ION PLANS*, 2008.

[21] W. L. Winkler and R. L. Hayes, Statistics: Probability, Inference, and Decision, 1st ed., Holt, Rinehart and Winston, inc., 1971.

[22] V. Levenshtein, "Binary codes capable of correcting deletions, insertions and reversals," *Soviet Physice -- Doklady ,* vol. 10, pp. 707-710, 1966.

[23] F. Damerau, "A technique for computer detection and correction of spelling errors," *Communications of the ACM,* vol. 7, no. 3, pp. 659-664, 1964.

[24] P. D. Groves and K. V. D. W. a. L. W. Henry Martin, "Context Detection, Categorization and Connectivity for Advanced Adaptive Integrated Navigation," in *ION GNSS+*, 2013.

[25] C. McManus, W. Churchill, A. Napier, B. Davis and P. Newman, "Distraction Suppression for Visual-Based Pose Estimation at City Scales," in *IEEE int. Conf. on Robotics and Automation*, 2013.

[26] J. Shockley and J. Raquet, "Three-axis magnetometer navigation in suburban areas," in *25th International Technical Meeting of The Satellite Division of the Institute of Navigation*, 2012.

[27] L. Wang, P. Groves and M. Ziebart, "Urban Positioning on a Smartphone: Real-time Shadow Matching Using GNSS and 3D City Models," in *ION GNSS+*, 2013.

[28] H. Martin, P. Groves, M. Newman and R. Faragher, "A New Approach to Better Low-cost MEMS IMU Performance Using Sensor Arrays," in *ION GNSS+*, 2013.